



OPEN

Intestinal preservation in a birdlike dinosaur supports conservatism in digestive canal evolution among theropods

Xuri Wang¹✉, Andrea Cau²✉, Bin Guo³, Feimin Ma³, Gele Qing³ & Yichuan Liu⁴

Dromaeosaurids were bird-like dinosaurs with a predatory ecology known to forage on fish, mammals and other dinosaurs. We describe *Daurlong wangi* gen. et sp. nov., a dromaeosaurid from the Lower Cretaceous Jehol Biota of Inner Mongolia, China. Exceptional preservation in this specimen includes a large bluish layer in the abdomen which represents one of the few occurrences of intestinal remnants among non-avian dinosaurs. Phylogenetically, *Daurlong* nests among a lineage of short-armed Jehol Biota species closer to eudromaeosaurs than microraptorines. The topographic correspondence between the exceptionally preserved intestine in the more stem-ward *Scipionyx* and the remnants in the more birdlike *Daurlong* provides a phylogenetic framework for inferring intestine tract extent in other theropods lacking fossilized visceral tissues. Gastrointestinal organization results conservative among faunivorous dinosaurs, with the evolution of a bird-like alimentary canal restricted to avian theropods.

Dromaeosauridae is a clade of small- to mid-sized theropod dinosaurs known from the Cretaceous of both hemispheres¹. The Lower Cretaceous Jehol Biota from north-eastern China has provided a rich diversity of dromaeosaurids, the majority of which referred to Microraptorialae^{2–7}. The affinities of two other Jehol Biota dromaeosaurids, *Tianyuraptor ostromi*⁶ and *Zhenyuanlong suni*⁷, are more problematic. These dromaeosaurids share some derived features with Microraptorialae⁷, yet they differ in having relatively shorter forelimbs and a larger body size, recalling other Laurasian dromaeosaurids (i.e., Eudromaeosauria¹). The abundance of Jehol Biota dromaeosaurids, when not due to taxonomic oversplitting¹, may be ecologically explained assuming niche segregation and avoidance of direct resource competition. This palaeoecological interpretation is supported by the diversity in body size, crano-dental and appendicular specializations reported in these taxa^{1–7}. Here, we describe a new dromaeosaurid from the Lower Cretaceous of the Pigeon Hill locality, Inner Mongolia (China), which shows the first case of intestinal preservation in a theropod lineage very close to bird ancestry.

Institutional abbreviation: IMMNH, Inner Mongolia Museum of Natural History, Hohhot, China.

Results

Systematic palaeontology. Dinosauria, Theropoda, Dromaeosauridae, *Daurlong wangi* gen. et sp. nov.

Holotype IMMNH-PV00731, an almost complete dromaeosaurid (Figs. 1, 2, Supplementary information). **Locality and Horizon** Pigeon Hill, Morin Dawa Daur Autonomous Banner, Inner Mongolia Autonomous Region (N 48°39'40.76"/E 123°52' 41.15"); Longjiang Formation, Lower Cretaceous.

Etymology The genus name is derived from the Daur Nation, and the Chinese 龙 ("lóng") for "dragon". The species name honors Mr. Wang Junyou, director of the IMMNH.

Diagnosis Mid-sized dromaeosaurid with (autapomorphies marked by asterisk): slender subnarial ramus of premaxilla extended caudally well beyond the external naris; large, trapezoid promaxillary recess placed at the rostroventral corner of antorbital fossa*; maxillary fossa large, shallow and caudodorsally located, so that the *pila promaxillaris* is wider than the *pila interfenestralis**; stepped transition from the subcutaneous surface of maxillary ventral ramus to the antorbital fossa; fan-shaped distal end of first sternal rib*. Differential diagno-

¹Key Laboratory of Stratigraphy and Paleontology of the Ministry of Natural Resources, Institute of Geology, Chinese Academy of Geological Sciences, Beijing 100037, China. ²Unaffiliated, 43125 Parma, Italy. ³Inner Mongolia Museum of Natural History, Huhhot 010010, Inner Mongolia, China. ⁴China University of Geosciences, Beijing 100083, China. ✉email: 147966459@qq.com; cauand@gmail.com

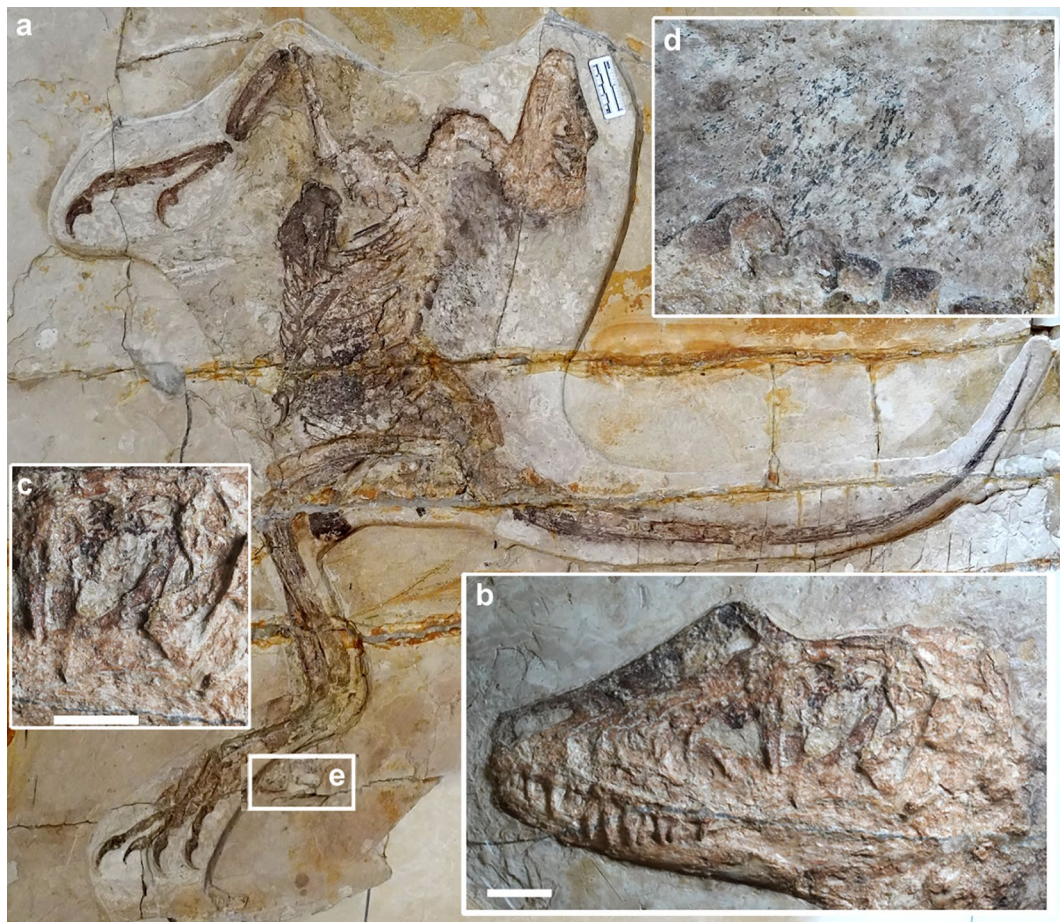


Figure 1. *Daurlong wangi* holotype. (a), whole specimen. (b), skull. (c), detail of orbit region. (d), feather remains associated to the thoracic vertebrae. (e), anuran skeleton. Scale bars: 20 mm (b), 10 mm (c).

sis: *Daurlong* further differs from *Tianyuraptor* because it bears longer and more robust maxillary teeth and a more robust ulna. *Daurlong* further differs from *Zhenyuanlong* because it lacks a pitted ventral ramus of the antorbital fossa, lacks markedly concave distal margins in maxillary tooth crowns, bears a bowed scapula, a more robust radius, and a wider overlap of the semilunate carpal over metacarpal II (Fig. 3).

Description and comparison. The holotype of *Daurlong wangi* is an almost complete and articulated skeleton with a length of about 150 cm (Fig. 1). Part of the ribcage and the corresponding gastralia region are overlapped by the left forelimb (segments of the humerus and forearm are missing) and suffered some crushing during diagenesis. The specimen is 85% the size of *Tianyuraptor ostromi* holotype⁶, 93% the size of *Zhenyuanlong suni* holotype⁷, and between 115 and 350% the size of the Jehol Biota microraptoriines^{5,8}. The skull is almost perfectly articulated, except for the missing nasal ramus of the left premaxilla and the partially displaced dorsal parts of the right nasal and lacrimal (Figs. 1, 3). A similar displacement of nasal and lacrimal is visible in the holotype of *Zhenyuanlong*⁷. The skull is about 94% of femur length, comparable to most taxa (e.g., *Halszkaraptor*, *Microraptor* and *Saurornitholestes*) whose skulls are approximately 92–95% of femur length^{8–13}. In *Zhenyuanlong*, the skull is about 86% of femur length⁷, and in *Tianyuraptor* the skull is longer than the femur⁶. In *Bambiraptor* and *Sinornithosaurus*, the skull is about 103–105% longer than the femur¹¹. In *Velociraptor*, the skull is between 117 and 128% of femur length, due to the relatively elongate snout¹⁰. The rostral margin of the premaxilla forms a right angle with the occlusal margin, similar to *Velociraptor*, *Zhenyuanlong* and *Saurornitholestes*^{2,10,12}, differing from the shallower premaxillae with acute rostroventral corner in *Microraptor* and *Sinornithosaurus*^{4,11} and the shallow platyrostral premaxilla of *Halszkaraptor*¹³. The subnarial process of the premaxilla extends caudodorsally well beyond the caudal margin of the external naris, as in *Velociraptor* and *Linheraptor*^{12,14}, differing from the relatively shorter processes in *Microraptor* and *Zhenyuanlong*^{2,5}. *Saurornitholestes* shows an intermediate condition. The external naris is relatively small, tear-shaped with the long axis directed caudodorsally, similar to *Zhenyuanlong*⁷ and differing from the relatively larger external naris in *Microraptor*⁴. In eudromaeosaurs, the external naris is relatively shorter and its long axis is subparallel to the oral margin^{10,12}.

The subcutaneous part of the rostral ramus of the maxilla is relatively small and triangular, taller than long and similar to *Zhenyuanlong*⁷ and *Wulong*¹⁵, differing from the relatively more elongate ramus in *Halszkaraptor*¹³, *Microraptor*⁴ and in some eudromaeosaurs^{14,16,17}. The antorbital fossa is large, longer than tall and covering

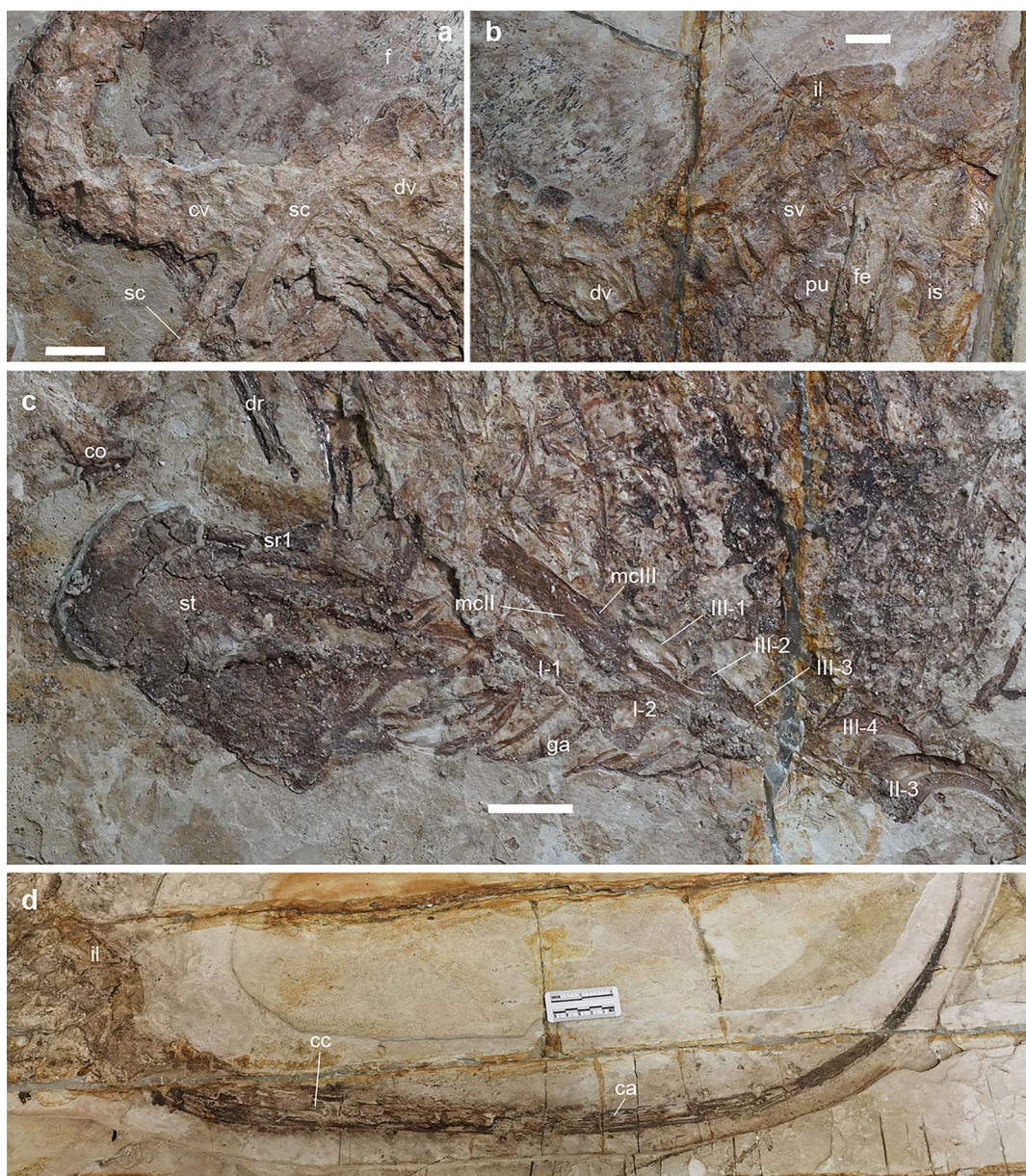


Figure 2. Selected elements of *Daurlong wangii* holotype. (a), neck and pectoral region. (b), thoraco-sacral series. (c), ventral part of the belly region. (d), tail. Abbreviations: ca, caudotheca; cc, caudal centrum; co, coracoid; cv, cervical vertebrae; dr, dorsal rib; dv, dorsal vertebrae; f, feathers; fe, femur; ga, gastralia; I-/II-/III-, phalanges; il, ilium; is, ischium; mc, metacarpal; pu, pubis; sc, scapula; st, sternum; sr1, sternal rib1; sv, sacral vertebrae. Scale bars in (a-c)=20 mm.

more than two-thirds of the maxilla, similar to *Zhenyuanlong* and *Wulong*^{7,15}, differing from the relatively shorter excavation seen in some eudromaeosaurs (e.g., *Acheroraptor*¹⁷). As in *Zhenyuanlong*, the rostral margin of the antorbital fossa is at the level of the second maxillary tooth, more rostral than in other dromaeosaurids^{4,7,12}. The promaxillary fenestra is relatively large, as in other Jehol Biota dromaeosaurids⁶ and is placed adjacent to the rostroventral corner of the antorbital fossa, differing from the more caudally placed fenestra in *Sinornithosaurus* and *Zhenyuanlong*^{7,11}. In *Microraptor*, the promaxillary fenestra is narrower rostrocaudally and elongated dorsoventrally⁴. The promaxillary fenestra is trapezoid in lateral view, with straight rostral, caudal and ventral margins, and a caudodorsally slanted dorsal margin. The maxillary recess is a large shallow fossa delimited by curved ridges paralleling the rostral margin of the antorbital fenestra. The *pila promaxillaris* is rostrocaudally wider than the *pila interfenestralis* (Supplementary information), a condition differentiating *Daurlong* from both *Tianyuraptor* and *Zhenyuanlong*, which show a relatively narrower *pila promaxillaris*^{6,7}. In microraptorines^{4,11} the area around the *pila promaxillaris* and the region underneath the antorbital fenestra are excavated by a series of small pits and ridges, absent in *Daurlong*. The caudoventral ramus of the antorbital fossa lacks the pits and crests present in *Zhenyuanlong*⁷. The dorsoventrally shallow subcutaneous surface of the ventral ramus is separated

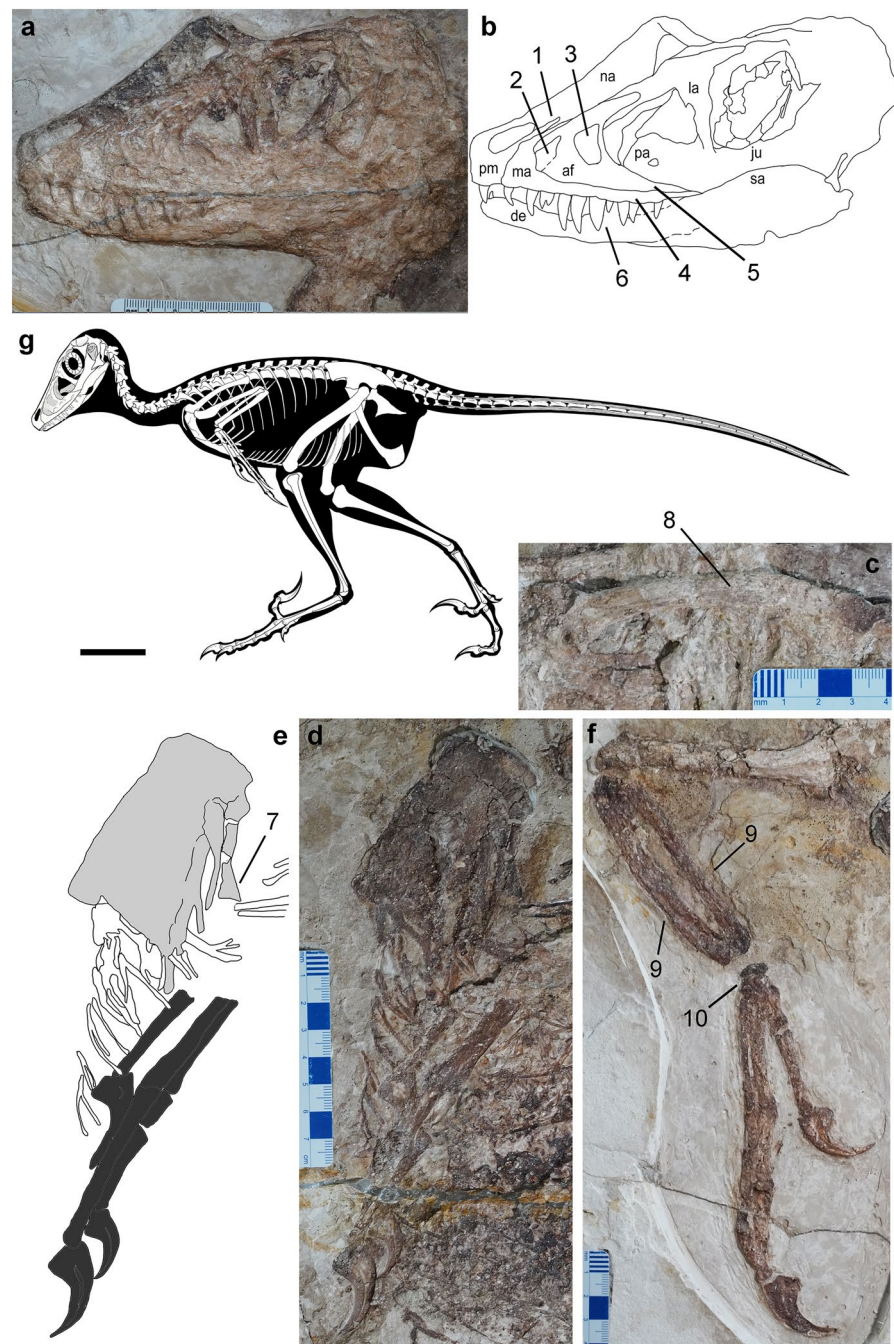


Figure 3. Diagnosis of *Daurlong wangii*. Specimen IMMNH-PV00731. Skull (a, b), left scapula (c), sternum and left hand (d, e), right forelimb (f). Reconstruction in (g) by M. Auditore (CC-BY 4.0). Combination of features diagnostic for *D. wangii*: 1, slender subnarial ramus of premaxilla extended caudally well beyond the external naris; 2, large, trapezoid promaxillary recess placed at the rostroventral corner of antorbital fossa; 3, maxillary fossa large, shallow and caudodorsally located, so that the *pila promaxillaris* is wider than the *pila interfenestrals*; 4, stepped subcutaneous surface of the ventral ramus of maxilla; 5, absence of pitted ventral ramus of the antorbital fossa; 6, robust fang-like maxillary teeth with straight to slightly convex distal crown margins; 7, distal end of first sternal rib fan-shaped. 8, bowed scapula; 9, radius and ulna more robust than any manual element; 10, wide overlap of the semilunate carpal over metacarpal II. In D, gray area indicates sternum, black areas indicate left hand elements. Abbreviations: af, antorbital fossa; de, dentary; ju, jugal; la, lacrimal; ma, maxilla; na, nasal; pm, premaxilla; su, surangular. Scale bar in G = 10 cm.

from the antorbital fossa by a stepped margin, differing from *Zhenyuanlong* which shows a distinct antorbital rim⁷. As in other dromaeosaurids^{17–19}, the postrantral wall is widely exposed in lateral view.

The lacrimal is T-shaped as in most dromaeosaurids^{4,10–12}. The frontal widely contributes to the dorsal margin of the orbit. The orbit is ovoid-shaped with the long axis directed rostroventrally-caudodorsally (Fig. 1). The scleral ring is nearly completely preserved inside the orbit. Its dorsoventral axis coincides with that of the orbital fenestra, and does not appear significantly deformed, allowing for an accurate measurement of its inner and external diameters. The scleral ring is large (external diameter about 93% of orbital diameter) and moderately slender. The rostral ramus of the postorbital is upturned, forming an obtuse angle with the caudal ramus, which is instead perpendicular to the ventral ramus. The elements of the caudal portion of the skull are badly preserved. The dentary shows a length/depth ratio of approximately 8, proportionally intermediate between the more gracile conditions in *Microraptor* and *Velociraptor*, and the relatively stouter dentary of *Saurornitholestes*^{4,10,12}. The dorsal margin is slanted rostroventrally at its rostralmost end, then, caudal to the second alveolus, it is parallel to most of the ventral margin, as in most non-dromaeosaurine dromaeosaurids^{4,10}. The ventral margin of the dentary gradually tapers rostrodorsally from the rostral sixth of the bone, and then is inclined caudodorsally along the caudal third. The postdentary elements of the mandible are badly preserved.

The single premaxillary tooth crown preserved is unserrated, bears a sharp apex, and is slightly curved distally near the apex. Ten teeth are preserved in the maxilla, with an additional tooth missing. The crowns are more robust and elongate than those of *Tianyuraptor*⁶. The middle maxillary teeth are the longest and fang-like, similar to those of *Microraptor*⁴. The crowns of the second, fourth and last preserved maxillary tooth bear dense serrations along their distal carinae. All maxillary teeth are blade-shaped and only slightly curved distally near the apex, differing from the more curved teeth of *Zhenyuanlong*⁷. Six dentary teeth can be recognized. They are much smaller than the maxillary teeth. Ten cervical vertebrae are preserved in articulation, but badly preserved (Fig. 2). The cranial neural spines of the dorsal series are rectangular and strongly inclined caudodorsally. The caudal neural spines of the dorsal series are square-shaped, with their long axis oriented dorsally, almost vertical to the corresponding centra (Fig. 2). The sacrum includes six vertebrae. The sutures along the sacral centra are obliterated, except for a faint suture visible between centra 2 and 3. The first caudal vertebra is similar in size to the last sacral vertebra. The tail is complete, approximately 4.4 times longer than the femur, but the number of the vertebrae is uncertain (Fig. 2). Most of the caudal vertebrae are encased in the caudotheca²¹ as in microraptorigines and eudromaeosaurs^{4,20}. *Daurlong* is similar to other Jehol Biota dromaeosaurids^{4,6,7} in having the caudotheca extended through the rostralmost vertebrae, differing from eudromaeosaurs where the bony rods bundle begins distal to caudal 6^{20,21}. The scapula is strap-like and uniformly bowed dorsally, differing from the straight scapula of *Zhenyuanlong*⁷. As in most paravians, the scapula is shorter than the humerus and more gracile than mid-shaft diameter of the ulna, with no distal expansion. The left coracoid is partially preserved. The bone is fused to the scapula, and both contribute to the laterally-facing glenoid, as in other paravians^{1,22}. There is no evidence of the large coracoid fenestra present in some microraptorigines^{4,4}. The sternum is large and subrectangular with the long axis as long as the humeral shaft (Fig. 2). It appears as a single unpaired element, as in *Microraptor*²¹, and differing from the incompletely fused elements in *Halszkaraptor* and eudromaeosaurs^{1,14,24}. Four pairs of sternal ribs articulate with the sternum, as in *Microraptor* and *Sinornithosaurus*, differing from *Zhongjianosaurus* which shows five pairs²⁵. The first pair of sternal ribs is more robust than the others and shows an elongate fan-shaped morphology expanded laterodistally, differing from the slender shaft and the spoon-shaped distal end shared by other dromaeosaurids^{5,25}. In some avialans²⁶, the caudalmost sternal rib is the most robust and shows an expanded distal end similar to the condition in *Daurlong*. As in other paravians, the gastralia contact the pubis shaft in a position more proximal than in other theropods, where instead such contact is usually placed on the pubic foot²⁷.

The forelimb length is less than 60% of the hindlimb. Among dromaeosaurids, comparably short forelimbs are shared with *Austroraptor*¹⁹, halszkaraptorigines⁹, *Tianyuraptor*⁶ and *Zhenyuanlong*⁷, and differ from the relatively longer forelimbs in *Buitreraptor*²⁸, microraptorigines^{4,5}, and some eudromaeosaurs²⁰. The deltopectoral crest is not prominently developed. The ulna is slightly bowed caudally and more robust than in *Tianyuraptor*⁶. The radial shaft is about half the thickness of the ulna and nearly equal to the mid-shaft of the manual phalanx I-1; in *Zhenyuanlong* the radius is apomorphically more gracile⁷. In the carpus, the stout scapholunare articulates distally with the semilunate carpal, which, in turn, overlaps the whole extent of the proximal end of metacarpal II, differing from the more limited overlap in *Zhenyuanlong*⁷. The combined metacarpal I + manual phalanx I-1 complex is longer than metacarpal II, differing from microraptorigines which have metacarpal II longer than metacarpal I + phalanx I-1^{4,5}. Manual digit II is the longest and bears the largest claw. As in microraptorigines and eudromaeosaurs^{4,5,20} manual phalanx III-2 is shortened, being about half the length of phalanx III-1. All the three recurved manual claws bear prominent flexor tubercles and horny sheaths. The ilium is 64% of the femoral length. The preacetabular process is longer than the postacetabular process of the ilium, a feature shared with *Halszkaraptor*, *Tianyuraptor* and *Unenlagia* among dromaeosaurids^{6,9,29}, and comparable to *Rahonavis* and most avialans³⁰. As in other dromaeosaurids⁵, the postacetabular process is gradually declined caudoventrally but does not extend below the level of the ischial peduncle. The pubic shaft is straight and caudoventrally oriented. The pubic foot is broadly rounded and dorsoventrally expanded, as in other Jehol Biota dromaeosaurids². The ischium is about half the pubis in length, lacks dorsal processes along the straight dorsal margin and ends distally in a poorly curved tip. The obturator process is triangular, as long as deep, and placed at mid-length of the ventral margin, differing from the prominent and more distally-placed process in microraptorigines⁵.

The femur is 91% of the tibia in length (in both *Tianyuraptor* and *Zhenyuanlong*, the femur is < 77% of the tibia). In theropods, the femur-to-tibia ratio is allometrically controlled³¹, and results higher in large-bodied dromaeosaurids than in small-bodied taxa³². The feet are incomplete, with the medialmost elements (i.e., toes I and II) badly preserved and overlapped by other foot bones. Metatarsal III and IV are nearly equal in length and about 61% of the femoral length. The preserved four pedal claws are comparable in size, are strongly recurved and bear low but prominent flexor tubercles.

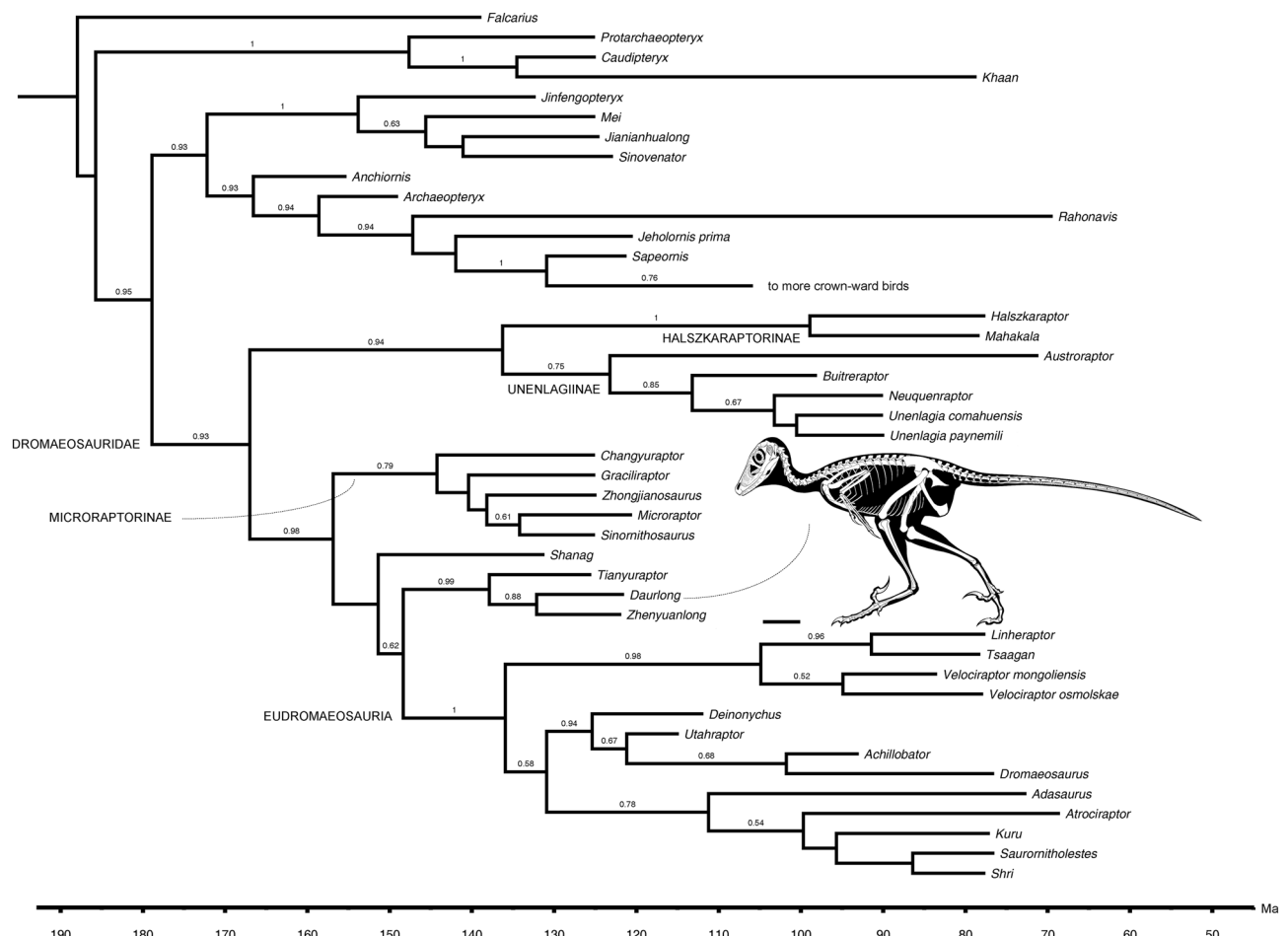


Figure 4. Affinities of *Daurlong wangi*. Time-calibrated Maximum Clade Credibility Tree reconstructed by the tip-dating Bayesian inference analysis. Values at branches indicate posterior probability. Scale bar = 100 mm. Skeletal drawing credit: Marco Auditore (CC-BY 4.0).

The plumage is preserved along the dorsal margin of the postorbital part of the skull, adjacent to the presacral neural spines (Fig. 1d) and along the edges of the tail. No feathers are preserved close to the limbs or along the ventral margin of the body: it is unclear if long pennaceous remiges and rectrices were present as in *Zhenyuanlong*⁷. The plumage along the dorsal margin of the pre-caudal part of the skeleton is preserved as a series of compound structures containing several filaments joined at their proximal ends, similar to the condition in *Sinornithosaurus*³³. Short pennaceous feathers are preserved along most of the margin of the caudotheca. The tail feathers appear symmetrical, oriented backward and forming a low angle (~ 15–20°) with the proximodistal axis of the adjacent tail vertebrae. Scanning electron microscopy (SEM) of sampled portions of the tegumentary remains failed to identify melanosomes^{34–36}. The caudal half of the abdominal cavity of the theropod is occupied by a black-bluish layer which is bound by the gastral basket (ventrally) and the pubis (caudally) (Figs. 1, 2, Supplementary Information). The rostral margin of the layer is placed ventral to the 9th dorsal centrum, where it extends dorsoventrally along the dorsal half of the abdominal cavity. The black-bluish layer reaches its maximum depth between the 10th and the 11th dorsal vertebrae, where it reaches the ventralmost part of the gastral basket. Caudal to the 11th dorsal vertebra, the layer is limited to the dorsal end of the abdominal cavity.

The imprint of the partial skeleton of an anuran is preserved in the same slab of IMNH-PV00731, adjacent to the theropod metatarsi (Fig. 1).

Discussion

Phylogenetic affinities of *Daurlong wangi*. *Daurlong wangi* is unambiguously referred to Dromaeosauridae based on the combination of large promaxillary recess^{4,11}, caudodorsally placed maxillary recess^{4,11,12}, tail with caudotheca²¹, shortened manual phalanx III-2^{4–7} and caudoventrally-oriented pubis with cup-shaped distal foot^{2–7}. It shows the closest phyletic affinity with *Tianyuraptor* and *Zhenyuanlong*^{6,7} (Fig. 4; Supplementary Information). In particular, *Daurlong* shares with these dromaeosaurids the antorbital region which is very extensive rostrally (resulting in a very short subcutaneous part of the preantorbital maxilla), a reduced deltopectoral crest of the humerus, and the elongation of the preacetabular process of the ilium^{6,7}. These three dromaeosaurids are significantly larger in body size than the other Jehol Biota paravians (e.g.,^{3,4}). *Daurlong* differs from *Tianyuraptor*

and *Zhenyuanlong* in the absence of accessory antorbital pits, in the robustness and curvature of the maxillary teeth, and in the relative robustness of the forearm elements. The relationships between the "*Tianyuraptor*-like" clade and their closest relatives are weakly-supported. This is likely due to the mosaic morphology of the "*Tianyuraptor*-like" taxa which combines features alternatively supporting close relationships with Microraptorinae or with Eudromaeosauria^{1,6}. It is noteworthy that the "*Tianyuraptor*-like" taxa retain features ancestral to both the above mentioned clades, shared with earlier-diverging dromaeosaurids (i.e., halszkaraptorines and unenlagiines) or with non-dromaeosaurid paravians (e.g., troodontids), such as the absence of a fossa bounding the maxillary recess^{4,18}, the relatively short forelimbs (i.e., shared with troodontids, halszkaraptorines and some unenlagiines^{9,19}), and the elongation of the preacetabular process of the ilium (i.e., shared with the halszkaraptorines, some unenlagiines, and avialans^{9,19}).

Conservatism in non-avian theropod gastrointestinal organization. The reconstruction of the gastrointestinal track in extinct taxa, including dinosaurs, could be inferred, indirectly, from gut content remains; less frequently by the analysis of coprolite contents; and rarely from exceptionally preserved remnants of the soft tissues^{37–48}. The topographic distribution of the bluish layer in the caudal half of the ribcage in IMMNH-PV00731 (Fig. 1, Supplementary Information) closely matches the extent of the intestinal track preserved in the non-avian theropod *Scipionyx*⁴¹. As in *Scipionyx* intestine, the bluish layer does not extend cranial to the 9th dorsal vertebra and shows its maximum dorsoventral extent at the level of the 10th–12th dorsal vertebrae, where it reaches the gastral basket. In both cases, an “empty” region separates the intestinal mass from the cranial margin of the pubis shaft⁴¹. At the micrometric scale, the bluish layer is formed by a fabric of densely packed microcrystals ranging 1–3 micron in diameter (Supplementary information), as in *Scipionyx* intestine⁴¹, suggesting that it represents the product of authigenic mineralisation⁴⁹ driven by the activity of decay bacteria, which replicated the large-scale outline of the decayed distal part of the gastrointestinal track⁴¹. Intestinal record in non-avian theropods is rare, occurring in *Scipionyx*⁴¹ and *Mirischia*⁵⁰. The close topographic correspondence between the intestinal tracks in *Daurlong* and *Scipionyx* relative to their axial skeletons might provide the basis for inferring the extent of the distal digestive region in other theropods bracketed phylogenetically by these taxa. Ovoid structures in the abdominal cavity of a specimen of *Sinosauropelta*, and argued to be eggs⁴², closely match in shape and position the duodenal portion of *Scipionyx* intestine⁴¹ and the ventral part of the bluish layer in *Daurlong*, and are here re-interpreted as intestinal remnants. The re-evaluation of the purported “eggs” of *Sinosauropelta* as intestinal portions is more in agreement with the skeletal immaturity of the specimen⁴² and dismisses an adult status for this compsognathid-grade theropod⁵¹. From an evolutionary perspective, the topographic correspondence between the whole intestinal mass in *Scipionyx* (considered an early-diverging coelurosaur⁴¹ or alternatively an allosauroid⁵¹) and the paravian *Daurlong* supports conservatism in intestinal general organization among faunivorous theropods. The evolution of a bird-like alimentary canal is thus inferred as an avian innovation⁴⁶. As in *Scipionyx*, the presence of intestinal remnants in *Daurlong* contrasts with the complete absence of any remnant of the stomach. Distinct taphonomic patterns, regulated by the physiological pH of the decaying organ, finely tuned the authigenic mineralisation: this process might had been inhibited by the persistence of the extremely acid environment of the stomach immediately after the death of the animal^{41,49}.

Methods

UV fluorescence photography. In order to identify any fluorescing minerals (e.g., calcium phosphate deposits, which discriminate preserved periosteal surfaces from eroded bones), the specimen was illuminated with a short wave UV lamp.

Scanning electron microscopy. Scanning electron microscopy (SEM) was obtained on samples removed from IMMNH-PV00731 with sterile dental tools, placed on carbon tape on copper stubs, sputter coated with Au and examined using a JEOL JSM-6700 and a ZEISS SIGMA-500 SEM at accelerating voltages of 15–20 kV.

Phylogenetic analyses. The phylogenetic affinities of the new dromaeosaurid were investigated scoring a taxonomic operational unit (OTU) based on IMMNH-PV00731 in a data set focusing on basal paravian and dromaeosaurid relationships. Character statement list was based on the data set of¹³ expanded with novel character statements described by¹⁸ (Supplementary information). Parsimony analysis was performed in TNT 1.5⁵² performing 100 ‘New Technology’ analyses followed by exploration of the sampled island using the ‘Traditional Search’ analysis. Nodal support was calculated sampling 10,000 trees up to ten steps longer than the shortest topologies (Supplementary information). Bayesian inference analyses integrating morphological and stratigraphic data were performed in BEAST 2.6^{53,54}, implemented with the packages for the analysis of morphological characters, using the model of⁵⁵, and for sampling potential ancestors among the ingroup⁵⁶. In our analysis, rate variation across traits was modeled using the multi-gamma parameter (implemented for the analysis of morphological data in BEAST 2). The rate variation across branches was modeled using the relaxed log-normal clock model, with the number of discrete rate categories that approximate the rate distribution set as n – 1 (with n the number of branches), the mean clock rate using default setting, and not setting to normalize the average rate. Since the character matrix includes autapomorphies of the sampled taxa, the model was not conditioned to variable characters only. Stratigraphic information for the taxa was converted to geochronological ages. Stratigraphic data and age constraints for each terminal were obtained from the Paleobiology Database (<http://paleobiodb.org/>), checked against the International Chronostratigraphic Chart (<http://stratigraphy.org/>), and included as uniform priors for tip-dating. The extant taxon included (the avian *Meleagris*) calibrates the height for the tip-date setting (the uniform prior setting used for incorporating uncertainty in the age of the fossil taxa

requires at least one terminal taxon to have the tip age fixed to a value⁵⁶). The analysis used one replicate run of 100 million generations, with sampling every 1000 generations. In the analyses, burnin was set at 40%. Convergence and effective sample sizes of every numerical parameter among the different analyses were identified using Tracer^{53,54}. The root age of the tree model was conservatively set as a uniform prior spanning between the age of the oldest in-group taxa and 200 Mya (near the Triassic-Jurassic boundary), which consistently pre-dates the diversification of all maniraptoran branches.

Nomenclatural act. This published work and the nomenclatural acts it contains have been registered in ZooBank, the online registration system for the ICBN. LSIDurn:lsid:zoobank.org:pub:9C845D24-3CC2-47CD-8993-E946C2D27D15.

Daurlong: LSIDurn:lsid:zoobank.org:act:28B9C1F5-665F-4517-81C1-25F7066D61F8.

Daurlong wangi: LSIDurn:lsid:zoobank.org:act:61,938,885-1854-4CCC-B723-C4065C83BEBA.

Data availability

All data generated or analysed during this study are included in this published article and its supplementary information files.

Received: 29 June 2022; Accepted: 17 November 2022

Published online: 19 November 2022

References

- Turner, A. H., Makovicky, P. J. & Norell, M. A. A review of dromaeosaurid systematics and paravian phylogeny. *Bull. Am. Mus. Nat. Hist.* **371**, 1–206 (2012).
- Xu, X., Wang, X. L. & Wu, X. C. A dromaeosaur dinosaur with filamentous integument from the Yixian Formation of China. *Nature* **401**, 262–266 (1999).
- Xu, X., Zhou, Z. & Wang, X. The smallest known non-avian theropod dinosaur. *Nature* **408**, 705–707 (2000).
- Pei, R., Li, Q., Meng, Q., Gao, K. Q. & Norell, M. A. A new specimen of *Microraptor* (Theropoda: Dromaeosauridae) from the Lower Cretaceous of western Liaoning, China. *Am. Mus. Novit.* **3821**, 1–28 (2014).
- Hwang, S. H., Norell, M. A., Ji, Q. & Gao, K. Q. New specimens of *Microraptor zhaoianus* (Theropoda: Dromaeosauridae) from northeastern China. *Am. Mus. Novit.* **3381**, 1–44 (2002).
- Zheng, X., Xu, X., You, H., Zhao, Q. & Dong, Z. A short-armed dromaeosaurid from the Jehol group of China with implications for early dromaeosaurid evolution. *Proc. R. Soc. B Biol. Sci.* **277**, 211–217 (2010).
- Lü, J. & Brusatte, S. L. A large, short-armed, winged dromaeosaurid (Dinosauria: Theropoda) from the Early Cretaceous of China and its implications for feather evolution. *Sci. Rep.* **5**, 1–11 (2015).
- Han, G. *et al.* A new raptorial dinosaur with exceptionally long feathering provides insights into dromaeosaurid flight performance. *Nat. Commun.* **5**, 4382 (2014).
- Cau, A. *et al.* Synchrotron scanning reveals amphibious ecomorphology in a new clade of bird-like dinosaurs. *Nature* **552**, 395–399 (2017).
- Currie, P. J. & Evans, D. C. Cranial anatomy of new specimens of *Saurornitholestes langstoni* (Dinosauria, Theropoda, Dromaeosauridae) from the Dinosaur Park formation (Campanian) of Alberta. *Anat. Rec.* **04715**, 1–25 (2019).
- Xu, X. & Wu, X. C. Cranial morphology of *Sinornithosaurus millenii* (Dinosauria: Theropoda: Dromaeosauridae) from the Yixian formation of Liaoning, China. *Can. J. Earth Sci.* **38**, 1739–1752 (2001).
- Barsbold, R. & Osmólska, H. The skull of *Velociraptor* (Theropoda) from the Late Cretaceous of Mongolia. *Acta Palaeontol. Pol.* **44**, 189–219 (1999).
- Cau, A. The body plan of *Halszkaraptor escutellie* (Dinosauria, Theropoda) is not a transitional form along the evolution of dromaeosaurid hypercarnivory. *PeerJ* **8**, e8672 (2020).
- Xu, X. *et al.* A new dromaeosaurid (Dinosauria: Theropoda) from the upper Cretaceous Wulansuhai Formation of Inner Mongolia, China. *Zootaxa* **2403**, 1–9 (2010).
- Poust, A. W., Gao, C. L., Varricchio, D. J., Wu, J. L. & Zhang, F. J. A new microraptorian theropod from the Jehol Biota and growth in early dromaeosaurids. *Anat. Rec.* **303**, 963–987 (2020).
- Godefroit, P., Currie, P. J., Hong, L., Shang, C. Y. & Dong, Z. M. A new species of *Velociraptor* (Dinosauria: Dromaeosauridae) from the upper Cretaceous of northern China. *J. Vertebr. Paleontol.* **28**, 432–438 (2008).
- Evans, D. C., Larson, D. W. & Currie, P. J. A new dromaeosaurid (Dinosauria: Theropoda) with Asian affinities from the latest Cretaceous of North America. *Sci. Nat.* **100**, 1041–1049 (2013).
- Powers, M. J. *et al.* A new hypothesis of eudromaeosaurian evolution: CT scans assist in testing and constructing morphological characters. *J. Vertebr. Paleontol.* **41**(5), e2010087 (2022).
- Novas, F. E., Pol, D., Canale, J. I., Porfiri, J. D. & Calvo, J. O. A bizarre Cretaceous theropod dinosaur from Patagonia and the evolution of Gondwanan dromaeosaurids. *Proc. R. Soc. B Biol. Sci.* **276**, 1101–1007 (2009).
- Ostrom, J. H. Osteology of *Deinonychus antirrhopus*, an unusual theropod from the lower Cretaceous of Montana. *Bull. Peabody Mus. Nat. Hist.* **30**, 1–165 (1969).
- Senter, P., Kirkland, J. I., DeBlieux, D. D., Madsen, S. & Toth, N. New dromaeosaurids (Dinosauria: Theropoda) from the lower Cretaceous of Utah, and the evolution of the dromaeosaurid tail. *PLoS ONE* **7**(5), 1–20 (2012).
- Brusatte, S. L. *et al.* The osteology of *Balaur bondoc*, an island-dwelling dromaeosaurid (Dinosauria: Theropoda) from the Late Cretaceous of Romania. *Bull. Am. Mus. Nat. Hist.* **374**, 1–100 (2013).
- Xu, X. *et al.* Four-winged dinosaurs from China. *Nature* **421**, 335–340 (2003).
- Cau, A., Beyrand, V., Barsbold, R., Tsogtbaatar, K. & Godefroit, P. Unusual pectoral apparatus in a predatory dinosaur resolves avian wishbone homology. *Sci. Rep.* **11**(14722), 1–10 (2021).
- Xu, X. & Qin, Z. C. A new tiny dromaeosaurid dinosaur from the lower Cretaceous Jehol Group of western Liaoning and niche differentiation among the Jehol dromaeosaurids. *Vert. PalAs* **55**, 129–144 (2017).
- Zheng, X. *et al.* Structure and possible ventilatory function of unusual, expanded sternal ribs in the Early Cretaceous bird *Jeholornis*. *Cretac. Res.* **116**, 104597 (2020).
- Rhodes, M. M. & Currie, P. J. The homology, form, and function of the microraptorian lateral pubic tubercle. *J. Vertebr. Paleontol.* **40**, e1755866 (2020).

28. Novas, F. E., Brissón Egli, F., Agnolín, F. L., Gianechini, F. A. & Cerdá, I. Postcranial osteology of a new specimen of *Buitreraptor gonzalezorum* (Theropoda, Unenlagiidae). *Cretac Res.* **83**, 127–167 (2018).
29. Novas, F. E., Agnolín, F. L., Motta, M. J. & Brissón, E. F. Osteology of *Unenlagia comahuensis* (Theropoda, Paraves, Unenlagiidae) from the Late Cretaceous of Patagonia. *Anat. Rec.* **304**, 2741–2788 (2021).
30. Forster, C. A., O'Connor, P. M., Chiappe, L. M. & Turner, A. H. The osteology of the Late Cretaceous paravian *Rahonavis ostromi* from Madagascar. *Palaeontol. Electron.* **23**(2), a31 (2020).
31. Holtz, T. R. The arctometatarsalian pes, an unusual structure of the metatarsus of Cretaceous Theropoda (Dinosauria: Saurischia). *J. Vertebr. Paleontol.* **14**(4), 480–519 (1994).
32. Perle, A., Norell, M. A. & Clark, J. M. A new maniraptoran theropod - *Achillobator giganicus* (Dromaeosauridae)-from the Upper Cretaceous of Burkhan, Mongolia. *Contributions of the Department of Geology, National University of Mongolia* **101**, 1–105 (1999).
33. Xu, X., Zhou, Z. H. & Prum, R. O. Branched integumental structures in *Sinornithosaurus* and the origin of feathers. *Nature* **410**, 200–204 (2001).
34. Zhang, F. et al. Fossilized melanosomes and the colour of Cretaceous dinosaurs and birds. *Nature* **463**, 1075–1078 (2010).
35. Li, Q. et al. Plumage color patterns of an extinct dinosaur. *Science* **327**, 1369–1372 (2010).
36. Li, Q. et al. Reconstruction of *Microraptor* and the evolution of iridescent plumage. *Science* **335**, 1215–1219 (2012).
37. Nesbitt, S. J., Turner, A. H., Erickson, G. M. & Norell, M. A. Prey choice and cannibalistic behaviour in the theropod *Coelophysis*. *Biol. Lett.* **22**(4), 611–614 (2006).
38. Charig, A. J. & Milner, A. C. *Baryonyx walkeri*, a fish-eating dinosaur from the Wealden of Surrey. *Bull. Nat. Hist. Mus.* **53**, 11–70 (1997).
39. Ostrom, J. H. The osteology of *Compsognathus longipes*. *Zitteliana* **4**, 73–118 (1978).
40. Xing, L. et al. Abdominal contents from two large early Cretaceous compsognathids (Dinosauria: Theropoda) demonstrate feeding on confuciusornithids and Dromaeosaurids. *PLoS ONE* **7**(8), e44012 (2012).
41. Dal Sasso, C. D. & Maganuco, S. *Scipionyx samniticus* (Theropoda: Compsognathidae) from the lower Cretaceous of Italy-osteology, ontogenetic assessment, phylogeny, soft tissue anatomy, taphonomy and palaeobiology. *Memorie (Museo Civico di Storia Naturale di Milano)* **37**, 1–281 (2011).
42. Currie, P. J. & Chen, P. J. Anatomy of *Sinosauroportex prima* from Liaoning, northeastern China. *Can. J. Earth Sci.* **38**, 1705–1727 (2001).
43. Varricchio, D. J. Gut contents from a Cretaceous tyrannosaurid; implications for theropod dinosaur digestive tracts. *J. Paleontol.* **75**, 401–406 (2001).
44. Zheng, X. T. et al. Exceptional dinosaur fossils reveal early origin of avian-style digestion. *Sci. Rep.* **8**, 1–8 (2018).
45. Dalsätt, J., Zhou, Z., Zhang, F. & Ericson, P. G. P. Food remains in *Confuciusornis sanctus* suggest a fish diet. *Sci. Nat.* **93**, 444–446 (2006).
46. Zheng, X. et al. New specimens of *Yanornis* indicate a piscivorous diet and modern alimentary canal. *PLoS ONE* **9**(4), e95036 (2014).
47. Xing, L. et al. Piscivory in the feathered dinosaur *Microraptor*. *Evolution* **67**, 2441–2445 (2013).
48. Chin, K., Tokaryk, T., Erickson, G. M. & Calk, C. A king-size theropod coprolite. *Nature* **393**, 680–682 (1998).
49. Briggs, D. E. G. The role of decay and mineralization in the preservation of soft-bodied fossils. *Annu. Rev. Earth Planet Sci.* **31**, 275–301 (2003).
50. Naish, D., Martill, D. M. & Frey, E. Ecology, systematics and biogeographical relationships of dinosaurs, including a new theropod, from the Santana Formation (?Albian, Early Cretaceous) of Brazil. *Hist. Biol.* **16**, 57–70 (2004).
51. Cau, A. Comments on the Mesozoic theropod dinosaurs from Italy. *Atti. Soc. Nat. Mat. Modena* **152**, 81–95 (2021).
52. Goloboff, P. & Catalano, S. TNT version 1.5. *Cladistics* **32**, 221–238 (2016).
53. Drummond, A. J., Suchard, M. A., Xie, D. & Rambaut, A. Bayesian phylogenetics with BEAUTi and the BEAST 1.7. *Mol. Biol. Evol.* **29**, 1969–1973 (2012).
54. Bouckaert, R. R. et al. BEAST 2: A software platform for Bayesian evolutionary analysis. *PLOS Comput. Biol.* **10**, e1003537 (2014).
55. Lewis, P. O. A likelihood approach to estimating phylogeny from discrete morphological character data. *Syst. Biol.* **50**, 913–925 (2001).
56. Gavryushkina, A., Welch, D., Stadler, T. & Drummond, A. J. Bayesian inference of sampled ancestor trees for epidemiology and fossil calibration. *PLOS Comput. Biol.* **10**, e1003919 (2014).

Acknowledgements

This work was supported by National Natural Science Foundation of China Grant 41872018, and China Geological Survey Grant DD20221649. We thank Marco Auditore (Associazione Paleontologica e Paleoartistica Italiana, Italy) for the iconographic support, and Valentina Rossi (University College Cork, Ireland) for suggestions on SEM analyses. We particularly thank Editor Sara Burch, Federico Agnolin (Museo Argentino de Ciencias Naturales "Bernardino Rivadavia") and an anonymous reviewer, whose comments significantly improved the quality of the manuscript.

Author contributions

X.W. led project administration, wrote the early draft. A.C. wrote the final draft, curated the data, performed the analyses, prepared the figures. B.G. studied the material, validated the results. F.M. studied the material, validated the results. G.Q. studied the material, validated the results. Y.L. studied the material, validated the results.

Competing interests

The authors declare no competing interests.

Additional information

Supplementary Information The online version contains supplementary material available at <https://doi.org/10.1038/s41598-022-24602-x>.

Correspondence and requests for materials should be addressed to X.W. or A.C.

Reprints and permissions information is available at www.nature.com/reprints.

Publisher's note Springer Nature remains neutral with regard to jurisdictional claims in published maps and institutional affiliations.



Open Access This article is licensed under a Creative Commons Attribution 4.0 International License, which permits use, sharing, adaptation, distribution and reproduction in any medium or format, as long as you give appropriate credit to the original author(s) and the source, provide a link to the Creative Commons licence, and indicate if changes were made. The images or other third party material in this article are included in the article's Creative Commons licence, unless indicated otherwise in a credit line to the material. If material is not included in the article's Creative Commons licence and your intended use is not permitted by statutory regulation or exceeds the permitted use, you will need to obtain permission directly from the copyright holder. To view a copy of this licence, visit <http://creativecommons.org/licenses/by/4.0/>.

© The Author(s) 2022